Performance of Poly(lactic acid)/ Cellulose Nanocrystal Composite Blown Films Processed by Two Different Compounding Approaches

Sonal S. Karkhanis[1], Nicole M. Stark,[2] Ronald C. Sabo,[2] Laurent M. Matuana[1]

[1] *School of Packaging, Michigan State University, East Lansing, Michigan*

[2] *U.S. Department of Agriculture, Forest Service, Forest Products Laboratory, One Gifford Pinchot Drive, Madison, Wisconsin*

This study was aimed to identify the best approach of incorporating cellulose nanocrystals (CNCs) into a poly (lactic acid) (PLA) matrix by examining two different CNC addition approaches. The first approach consisted of melt-blending (MB) PLA and CNCs in a three-piece internal mixer whereas the second method involved direct dry-mixing of PLA and CNCs in a high intensity mixer. The compounded materials were then blown into films and compared in terms of particle dispersion, optical, thermal, molecular weight and barrier properties. Good distribution was achieved by both the direct dry- and MB methods. However, some agglomerations were still present that resulted in reduced transparency of the composite films. Furthermore, the PLA/CNC films thermally degraded during the blending processes indicated by the drop in their molecular weights due to chain scissions. More chain scissions occurred in melt-blended (MB) films than the dry-blended (DB) counterparts. The addition of only 1% CNCs into the PLA matrix by the direct dry- and MB approaches improved the water barrier properties of PLA films by 30% and 24%, and oxygen barrier properties by 60% and 39%, respectively. The inferior performance of the MB films compared to the direct DB counterparts could be attributed to more chain scissions in these films. Thus, the direct dry-blending (DB) process appeared to be the better approach of incorporating CNCs into the PLA matrix. POLYM. ENG. SCI., 58:1965-1974, 2018. © 2017 Society of Plastics Engineers

INTRODUCTION

Growing concerns about sustainability, environmental awareness and government policies are driving industries and researchers to develop bio-based and biodegradable materials [l]. Poly(lactic acid) (PLA), a thermoplastic derived from renewable resources such as starch from com and potatoes, is an eco-friendly polymer that can provide an attractive solution to mounting concerns [2-12]. PLA has several desirable properties such as high stiffness, reasonable strength, excellent flavor and aroma barrier, as well as good grease and oil resistance. It has been extensively used as implants in biomedical applications and to manufacture rigid containers for food and consumer goods packaging. However, its widespread applicability in flexible films is limited due to its poor water and oxygen barrier properties, low impact strength and brittleness [2-12].

Cellulose nanomaterials such as cellulose nanocrystals (CNC) are often added to the PLA matrix to overcome few of its drawbacks [13-16]. For instance, well-dispersed nanocrystals can improve PLA's mechanical properties by improving stress transfer from the matrix to the CNCs [17]. Additionally, CNCs can act as nucleating agents to increase PLA's crystallinity [15-17]. Increased crystallinity is known to improve the barrier properties of materials because of the increase in packing efficiency of polymer chains, leading to a decrease in free volume [2, 18]. However, the dispersion of CNCs into a polymer matrix is a challenge. CNC particles tend to agglomerate due to their high surface area to volume ratio when the aqueous medium that they are produced in is eliminated by freeze or spray drying. Moreover, CNC particles are difficult to disperse in non-polar polymers due to their high polarity and strong hydrogen bonding forces [15, 16]. Various approaches, such as solvent casting and melt-compounding, have been investigated to disperse nanocelluloses into a polymer matrix [14, 18-23].

Recently, Pei and co-workers investigated the dispersion of chemically modified CNCs into a PLA matrix [19]. In this work, a predetermined amount of silylated CNC (SCNC) was dispersed in an organic solvent and mixed with a previously prepared solution of PLA. The mixture was stirred, casted on a glass petri dish and dried to form PLA/SCNC nanocomposite films. High degree of SCNCs' dispersion was achieved into the PLA matrix due to fiber treatment that reduced agglomeration. The PLA/1% SCNC films had higher crystallinity compared to the PLA films, leading to a 27% increase in tensile modulus. However, the elongation at break of the PLA/1% SCNC films was significantly lower than that of PLA films due to the poor interfacial adhesion between the PLA and nanoparticles resulting in insufficient stress transfer [19]. In another study, Fortunati and co-workers reported a reduction of 34% in water vapor permeability of PLA when 1% CNC modified with an acid phosphate ester of ethoxylated nonylphenol was added to the PLA matrix using the solvent casting technique [18].

PLA/cellulose nanofiber (CNF) composites have also been prepared using a two-step process [14]. The solvent casting technique was used to prepare a master batch, which was then crushed, diluted and dry-mixed with PLA, melt-compounded in an extruder, pelletized and finally injection molded. The *PLA/* 5% CNF samples prepared by the described technique had 24% and 21% increase in tensile modulus and tensile strength, respectively. Nonetheless, large standard deviation in the values

Correspondence to: L.M. Matuana; e-mail: matuana@msu.edu

Part of the results of this study have been presented at the 75th Annual Technical Conference of the Society of Plastics Engineers, held in Anaheim, California in May 2017.

Contract grant sponsor: The U.S. Endowment for Forestry and Communities, Inc. - The Public-Private Partnership for Nanotechnology; contract grant number: P3Nano Grant No. P3-8b

DOI 10.1002/pen.24806

Published online in Wiley Online Library (wileyonlinelibrary.com).

of tensile modulus reported indicated a non-homogenous dispersion of CNFs in the PLA matrix [14].

Another approach to disperse CNFs into a PLA matrix has been examined by other investigators who prepared aqueous suspensions of CNF in a slurry of plasticizer, acetone and water [20]. The prepared suspension was melt-compounded with PLA pellets in a twin-screw extruder equipped with a liquid feeder and vents for removal of acetone and water. The obtained extrudate was then compression molded into films for testing of mechanical properties. The results indicated that addition of only 1% CNF increased the elongation at break of the plasticized PLA by 27% due to the slippery effect of CNFs coated with plasticizer and the crazing phenomenon attributed to the presence of CNFs [20].

In a more recent study, PLA and 1% cellulose nanocrystal as well as chitin nanocrystal (ChNC) nanocomposite films were obtained using liquid feeding in a vented twin-screw extruder prior to compression molding [21]. A plasticizer (20% triethyl citrate [TEC]) was used to liquid feed the two types of nanocrystals while acting as a processing aid to enhance their dispersion into the PLA matrix. This liquid feeding technique resulted in moderate dispersion of CNCs as well as ChNCs in the PLA matrix, with some amount of agglomerations still present for both types of nanocrystals. However, significant increase in the yield strength (316% for CNCs and 478% for ChNCs) as well as Young's modulus (267% for CNCs and 300% for ChNCs) were obtained for the nanocomposite films compared to their counterpart PLA/TEC films without any nanocrystals [21].

The above-described liquid feeding approach has also been successfully used to produce plasticized PLA/polybutylene adipate-co-terephthalate (PBAT) blown films with talc and ChNC [22]. In this study, a masterbatch of PLA, 5% ChNCs and 20% glycerol triacetate plasticizer (GTA) was prepared using the previously described liquid feeding technique in a vented twin-screw extruder. This masterbatch was diluted with PLA and PBAT and mixed with talc to produce films with 1% ChNCs, 6% talc, 9% GTA, 25% PBAT, and 59% PLA. The final composites were then blown into films and evaluated for optical, thermal, mechanical and barrier properties amongst others. The researchers found that addition of ChNCs increased the viscosity and melt strength of PLA, thus aiding in the blown film processing. Moreover, the addition of 1% ChNCs increased the tensile modulus, tensile strength, tear resistance and puncture resistance of the film by 74%, 64%, 80%, and 300%, respectively. In contrast, the nanocomposite films did not have improved thermal stability or barrier performance compared to their reference films [22].

Processing aids such as polyvinyl alcohol (PVOH) have also been used to improve the dispersion of CNCs into the PLA matrix [23]. Enhanced dispersion of CNCs into PLA can be achieved by reacting the hydroxyl groups in PVOH with the hydrophilic CNCs and the vinyl acetate groups with the hydrophobic PLA. In one study, PLA/CNC nanocomposites were manufactured using PVOH by two different feeding methods: dry feeding PVOH/CNC pellets with PLA and liquid feeding PVOH/CNC suspension into molten PLA during extrusion in a vented twin-screw extruder. The composite materials were then compression-molded into films prior to testing for dispersion and mechanical performance. The results showed that poor interfacial adhesion between PLA and PVOH resulted in phase separation with a continuous PLA phase and discontinuous PVOH phase, irrespective of the feeding method. Furthermore, the CNCs were dominantly present in the PVOH phase due to their higher affinity to PVOH than PLA. Consequently, the nanocomposite films had poor mechanical properties due to the immiscibility of PLA and PVOH resulting in phase separation [23].

Although good nanoparticle dispersion into PLA matrix was reported by different solvent casting and liquid feeding techniques, these have various drawbacks [14, 17-20]. Solvent blending and casting techniques require drying of films, which add more energy consumption in film manufacture, and solvent disposal could also be an issue for this process because some solvents may be harmful to workers and the environment. Additionally, trace amounts of solvents can remain in the produced films, which could pose regulatory compliance issues. The residual solvent can also act as a plasticizer, thereby reducing the strength, stiffness and barrier properties of the produced films [24].

Due to the drawbacks of solvent-based mixing techniques, alternative approaches to manufacture PLA/CNC composite films should be considered. This study examined two solvent-free approaches of adding CNCs into the PLA matrix. The first approach was to melt-blend CNCs with PLA in a three-piece internal batch mixer to maximize homogenous dispersion of CNCs into the matrix while minimizing the loss of CNCs that may occur in high volume mixers [25]. Although this technique eliminates the use of solvents, it is a time-consuming batch process that subjects heat-sensitive PLA to additional thermal history. Therefore, a second approach employing conventional direct dry-blending (DB) was also examined. In this method, CNCs were directly added to the PLA matrix during conventional dry-compounding. Compared with melt-blending (MB), this less time-consuming approach minimizes exposure of PLA to high temperature.

To the best of our knowledge, these investigated blending approaches have not been previously used to manufacture PLA/CNC composite blown films. Consequently, the goal of this study was to compare the performance of PLA/CNC blown films prepared by the MB and direct DB techniques in terms of particle dispersion, optical, thermal, molecular weight and barrier properties to identify the most effective blending approach.

EXPERIMENTAL

Materials

Poly(lactic) acid (PLA 4044D) with a melt flow rate of 3.95 g/10 min (190°C, 2.16kg) and density of 1.24 g/cm^3, obtained from NatureWorks LLC (Minnetonka, MN) was used as the resin in this study. Freeze-dried cellulose nanocrystals were obtained from Forest Products Laboratory (2012-FPL-CNC-043). These CNCs were produced by dissolving wood pulp using the sulfuric acid process with a procedure described elsewhere (26]. They have diameters around 5 nm and lengths around 100-300nm [27].

Preparation of PLAICNC Composites

The CNCs were pre-blended in a high intensity mixer at 22,000 rpm for ~1 min to reduce their size from the received cake to a fine powder. PLA pellets and CNCs were oven-dried at 50°C for at least 24hr to remove moisture before compounding through the following two different approaches of incorporating CNCs into the PLA matrix.

 DOI 10.1002/pen

Melt-Blending Process (MB). Mixing temperature, speed and time affect the dispersion of additives into polymer matrices [28]. Blending of CNCs with PLA took place in an electrically heated 60ml three-piece internal mixer/measuring head (3:2 gear ratio) with counter-rotating roller style mixing blades (C.W. Brabender Instruments, South Hackensack, NJ) at 160°C for 3 min with the rotor speed set at 30rpm. A 5.6-kW (7.5hp) Intelli-Torque Plasti-Corder Torque Rheometer (C.W. Brabender Instruments, South Hackensack, NJ) powered the mixer. These processing conditions were optimized in our preliminary study. The CNC loading was fixed at 1 wt%, which was determined as the ideal concentration from our previous study [2]. The compounded materials were frozen for at least 24 hr and then pulverized using a Thomas-Wiley Laboratory Mill-Model 4 (A.H. Thomas Co., Philadelphia, PA) with a screen mesh size of 2 mm and then blown into a film as described in the following sections.

Direct DB. The direct DB of 1 wt% CNCs into PLA was carried out in a high intensity mixer at 22,000 rpm for ~ 1 min. The compounded materials were then used to manufacture blown film as described below.

Film Manufacturing

Neat PLA pellets and the compounded materials (CNC filled PLA processed by direct DB and MB) described above were blown into films using a 19mm single screw extruder (C.W. Brabender Instruments, South Hackensack, NJ), powered by a 3.73kW (5hp) Prep Center D52 (C.W. Brabender Instruments, South Hackensack, NJ). The extruder had a length-to-diameter ratio of 30:1 and was fitted with an annular die of diameter 25.4 mm and die opening of 0.889mm. A venting single-stage mixing screw (2.63:1 compression ratio) with a torpedo screw tip (35°) was used during processing. Starting from the hopper to the die, the temperature profile of the extruder was set at 180°C-180°C-180°C-180°C. The rotational screw speed of the extruder was set at 35 rpm whereas the speed of take-up rollers for drawing the film upward was set at 40rpm. An internal air pressure of 0.517kPa (0.075psi) was used to inflate the film. The blow-up ratio of the film, defined as the ratio of the diameter of the final tubular film to the diameter of the annular die, was calculated as 5. The average thickness was measured as ~0.027mm at 10 random locations along the film using a digital micrometer (model 49-70 from TMI, Ronkonkoma, NY) with a resolution of 0.001mm [2].

Property Evaluation

Differential Scanning Calorimetry (DSC). DSC was performed on the prepared films using a QlO0 instrument (TA Instruments, New Castle, DE) in accordance with ASTM D3418. The DSC cell was purged with liquid nitrogen flowing at 70 ml/min. Each test employed 6-10 mg of sample tested with a set of heating and cooling cycles. The samples were heated from 25°C to 200°C at a ramp rate of l0°C/min and held at 200°C for *5* min to erase their thermal history. Subsequently, the samples were cooled to 25°C and reheated to 200°C at the same ramp rate. The glass transition temperature (T_g), cold crystallization temperature (T_c), melt peak temperature (T_m), enthalpy of the cold crystallization process (ΔH_c) and melting peaks (ΔH_m) were determined using the software Universal Analysis 2000, V4.5 (TA Instruments, Delaware). The percentage crystallinity (% χ_c) was calculated from both, the first and second heat scans using the following *Eq.* [10, 29]:

$$\%\chi_c = \frac{\Delta H_c - \Delta H_m}{\Delta H_m^{\infty} \times [1 - (\%\text{wt CNC}/100)]} \times 100 \quad (1)$$

where %wt CNC is the total weight percentage of CNC (1 wt%). The melt enthalpy of a spherulite of infinite size (ΔH_{∞}) used for PLA was 93 J/g [6, 10, 29]. Six samples were tested for each material.

Thermogravimetric Analysis (TGA). Non-isothermal and isothermal TGA measurements of the neat PLA and PLA/CNC composite films were performed using a Q500 thermogravimetric analyzer (TA Instruments, New Castle, DE) on samples weighing between 6 and 10mg. For non-isothermal TGA, the samples (in triplicates) were heated from 25°C to 700°C at a ramp rate of 10°C/min under nitrogen atmosphere (40ml/min). In contrast, the samples were heated to l 80°C at a rate of 180°C/min and held isothermal for 300min under the same nitrogen atmosphere for isothermal TGA.

Gel Permeation Chromatography (GPC). The number average molecular weight (Mn), weight average molecular weight (M_w), and viscosity average molecular weight (Mv) of the PLA and PLNCNC composite films were measured by GPC instrument (Waters 1515, Waters, Milford, MA). The instrument was equipped with a series of HR Styragel columns (HR4, HR3, HR2 [300mm length by 7.8mm internal diameter]) and a refractive index detector (Waters 2414, Waters, Milford, MA). The test was conducted at a flow rate of 1 ml/min at 35°C using the Mark-Houwink corrected constant K=0.000174ml/g and α = 0.736 for PLA solution in tetrahydrofuran (THF). Polystyrene standards ranging between 2.9 X 10^3 and 3.64 X 10^6 daltons were used for calibration. Approximately 20 mg of sample was dissolved in 10ml of 99.99% pure THF. The samples were then filtered and transferred into 2ml glass vials. A syringe was used to inject 100 µl samples from the vial into the GPC. The detector and column were maintained at 35°C. The obtained data was analyzed using the Breeze software (version 3.30 SPA, 2002; Waters, Milford, MA). Seven samples were tested for each material.

Ultraviolet-Visible (UV-Vis) Spectroscopy. A UV-Vis spectrophotometer Perkin-Elmer Lambda 25 (Perkin-Elmer Instruments, Beaconsfield, UK) was used to record the transmittance of PLA and PLA/CNC composite films. The UV-Vis spectra were obtained over a wavelength range of 200-900 nm at a scan rate of 240nm/min. For each spectrum, the average light transmission value reported was estimated by averaging the percent light transmission values in the visible range, that is, from 380 to 720 nm wavelength. Three replicates were tested.

Fourier Transformation Infrared (FTIR) Spectroscopy. Infrared spectra of PLA and PLNCNC composite films were collected using a Shimadzu IR Affinity 1S infrared spectrophotometer (Shimadzu Corporation, Kyoto, Japan) to verify their mechanism of degradation. Each spectrum was obtained with triangle apodization using 64 scans in the range of 4000-400 cm^{-1}, at a wavelength resolution of 4 cm^{-1}. Films of similar thickness

(~0.018mm) were dried for 24hr in an oven at 50°C prior to testing. The thickness of samples was kept constant to allow comparison of different spectra since the peak intensity of a FTIR absorption band is dependent on the path length of infrared light, that is, sample's thickness.

The peak heights (peak intensity) were analyzed without smoothening or baseline correction. The peak intensity at 957 cm^{-1}, assigned to the O-H vibrations in carboxyl groups, a potential product of chain scission of PLA, was chosen to calculate the carboxyl index for each film [30, 31]. This peak was normalized using the intensities of reference peaks at 2994 and 2945 cm^{-1}, corresponding to stretching vibrations of C-H in saturated hydrocarbons, because they changed the least during thermal degradation due to processing. The carboxyl index for each film was calculated using the following *Eq.* [30, 31]:

$$\text{Carboxyl index} = \frac{I_{957}}{I_x} \quad (2)$$

where I_{957} is the peak intensity at 957 cm^{-1} and I_x is the peak intensity of reference peak at 2994 or 2945 cm^{-1}. Samples were tested in triplicates.

Light Microscopy. PLA and PLA/CNC composite films were observed using an Olympus BX41 optical microscope (Olympus, Center Valley, PA) equipped with a camera (Olympus Qcolor3).

Water Vapor Transmission Rate (WVTR) and Oxygen Transmission Rate (OTR). The WVTR of PLA and PLA/CNC composite films was measured in accordance with the desiccant method in ASTM E 96, as described previously [2]. Ten replicates of films manually cut and sealed onto 3/4" depth vapometer cup assemblies (Towing-Albert Instrument Co., West Berlin, NJ) were placed in a controlled humidity chamber (Model LH 1.5 from Associated Environmental Systems, Ayer, MA) set at 38°C and 85% relative humidity (RH). The inside of the cups was maintained at ~0% RH by using a desiccant (anhydrous calcium sulfate). The cups were periodically weighed to the nearest 0.0001 g for determining the weight gain as a function of time. The slope of the linear portion of weight gain versus time plots was used to calculate the WVTR, using the following *Eq.*:

$$\text{WVTR} = \frac{(W/t)}{A} \quad (3)$$

where W is the weight gain at time t, A is the effective area of exposed film (31.67 x 10^{-4} m^2), and W/t is the slope of the straight line.

OTR was measured using Ox-Tran Module 2/21 (Macon Inc, Minneapolis, MN), in accordance with the procedures outlined in ASTM D3985, as described previously [2]. At least six replicates for each film were tested at 23°C and 0% RH.

Statistics. Means were compared by the analysis of variance (ANOVA) and Tukey's honestly significant differences tests at *5%* level of significance using IBM SPSS Statistics 22 (Armonk, NY).

RESULTS AND DISCUSSION

Effect of Blending Process on CNC Dispersion and PLA's Optical Properties

CNC distribution and dispersion in the PLA matrix were examined using light microscopy (Fig. 1). In this study, CNC dispersion was defined as the degree of breaking up of CNC agglomerates, whereas CNC distribution was a measure of how uniformly the CNCs were distributed throughout the PLA matrix [32]. As seen in Fig. 1, homogenous distribution of CNCs in the PLA matrix was achieved, irrespective of the blending technique. However, some agglomerates were still visible, indicative of not well-dispersed CNCs in the matrix. The difference in CNC dispersion in the direct dry-blended (DB) and melt-blended (MB) films was not apparent from the obtained images. Therefore, UV-Vis spectroscopy was performed to further investigate the dispersion of CNCs into the PLA matrix (Fig. 2). Transparency can be used as an indicator of the dispersion of nanoparticles in a matrix, if the size of individual nanoparticles is smaller than the wavelength of visible light (380-700 nm) [20]. In other terms, if nanosize dispersion of CNC in PLA matrix is obtained, the addition of CNCs will not affect the transparency of resulting films, because pure CNC films are highly transparent [33]. The UV- Vis spectroscopy results for neat PLA and PLA/CNC composite films prepared by the direct DB and MB approaches are illustrated in Fig. 2. The average light transmission values for neat PLA, PLA/CNC direct DB and PLA/CNC MB films in the visible region were calculated as described in the experimental section and reported as 91.5% ± 0.8%, 78.5% ± 3.3%, and 74.5% ± 0.9%, respectively. These results show that the light transmission of neat PLA decreased significantly by adding 1% CNCs, irrespective of the blending technique (Fig. 2). Reduced transparency of PLA due to the addition of CNCs, irrespective of the blending method, implied that nanoscale dispersion did not fully occur and some micrometer sized agglomerations could still be present. The light microscope images showing agglomerations of CNCs

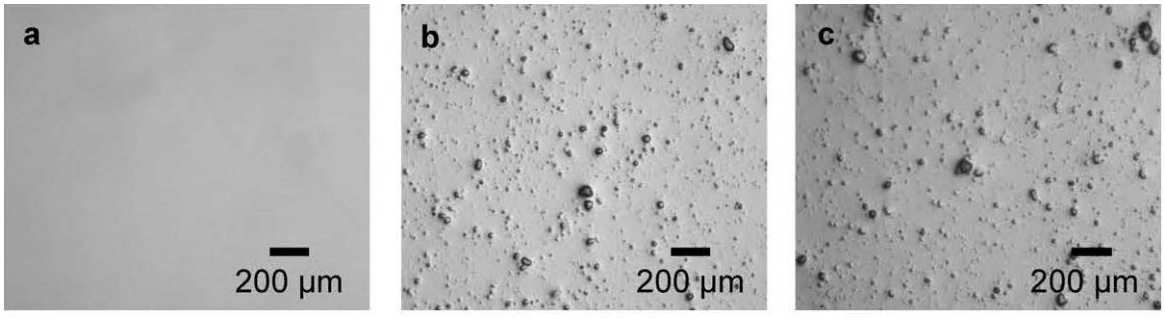

FIG. 1. Light microscope images of (a) PLA, (b) PLA/1% CNC (DB), and (c) PLA/1% CNC (MB) films.

 DOI 10.1002/pen

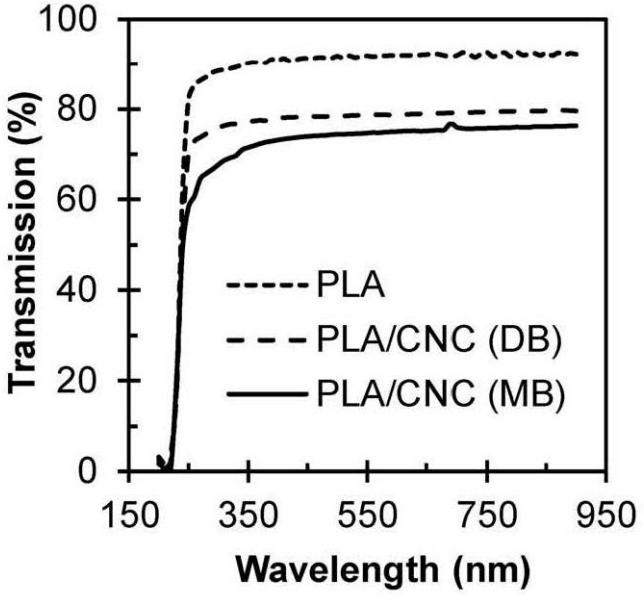

FIG . 2. Effects of CNC addition and blending process on the transparency of PLA and PLNCNC composite films.

(Fig. 1) corroborate the UV-Vis results (Fig. 2). Generally, nanoparticle agglomeration sizes larger than the incident wavelength of light tend to scatter light and reduce light transmission [20]. Although there is still need for improvement to completely eliminate agglomerations, a transparency in the range of 75%-78% was achieved in this study, demonstrating that reasonably good transparency remains despite limited dispersion. It is worth mentioning that the difference in average light transmission values of direct DB PLNCNC films (78.5% ± 3.3%) and MB PLNCNC films (74.5% ± 0.9%) were not significantly different, implying that blending methods yielded films of similar transparency.

Effects of CNC Addition and Blending Process on PLA's Thermal Properties

TGA was performed to evaluate the effects of CNC addition and blending approaches on the thermal decomposition of PLA. The non-isothermal TGA and differential thermogravimetric (DTG) curves of PLA and PLNCNC composite films are illustrated in Fig. 3a and b. There was no noticeable significant difference in the onset temperatures of decomposition (~315°C) measured on addition of 1% CNCs, irrespective of the blending process used. Similar results were reported by Lizundia and coworkers for PLA-grafted CNCs at 1 wt% [34]. It is evident from Fig. 3a that the decomposition of all films started at temperatures of ~315°C and reached their maximum decompositions at ~364°C. The decomposition of PLA above 200°C has been reported by various researchers and could be attributed to hydrolysis of ester bonds in the main chain, unzipping depolymerization reactions catalyzed by residual polymerization catalysts, oxidative random main-chain scission as well as inter and intramolecular transesterification reactions leading to the formation of low molecular weight monomers and oligomeric esters [12, 35-37]. Figure 3c shows the TGA measurements performed under isothermal conditions at 180°C for 300min for PLA and PLNCNC nanocomposite films. The addition of CNCs by both the direct DB and MB processes did not affect the decomposition of PLA films at the processing temperature used in this study to manufacture blown films. The weight loss for all films

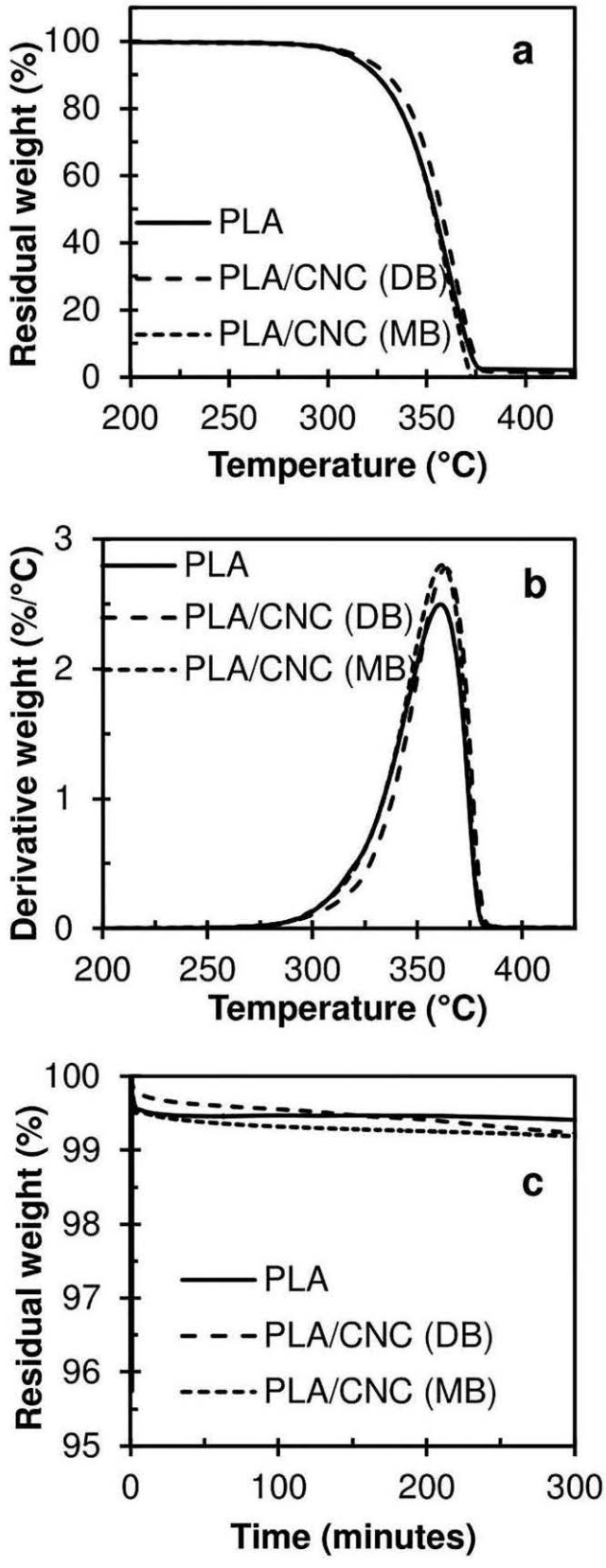

FIG. 3. (a) Non-isothermal thermograms, (b) non-isothermal DTG, and (c) isothermal thermograms of PLA and PLNCNC composite films.

TABLE 1. DSC analysis for PLA as well as direct dry-blended (DB) and melt-blended (MB) PLA/1% CNC films.

	T_g (°C)		T_c (°C)		T_m (°C)		χ_c (%)	
Materials	First heat	Second heat	First heat	Second heat	First heat	Second heat	First heat	Second heat
PLA	63.2 ± 2.9[a]	61.0 ± 0.4[a]	117.0 ± 3.1[a]	124.9 ± 1.2[a]	149.9 ± 0.3[a]	151.0 ± 0.5[a]	4.5±0.1[a]	1.5± 0.4[a]
PLA + 1% CNC (DB)	63.3 ± 3.0[a]	60.8 ± 0.2[a]	113.9 ± 2.1[b]	122.7 ± 1.2[b]	149.2 ± 0.3[a]	150.4 ± 0.4[a]	5.4 ± 0.8[b]	4.5 ± 0.4[b]
PLA + 1% CNC (MB)	64.5 ± 0.3[a]	61.1 ± 0.7[a]	111.7 ± 0.2[c]	113.2 ± 0.1[c]	147.7 ± 0.2[b]	148.0 ± 0.1[b]	4.6 ± 0.3[a]	4.4 ± 0.2[b]

Same superscript letters within the same column are not significantly different based on the ANOVA results at 5% significance level.

was around 1% even after holding the films at 180°C for 300min.

Table 1 lists the thermal transition temperatures (T_g, T_c, and T_m) and degree of crystallinity (%xc) from the first and second DSC heating scans measured for PLA as well as PLA/CNC composite films manufactured by the direct DB and MB techniques. In this study, the first heating scan was used to assess the film's thermal properties in the as-blown condition whereas the second heating scan was used to evaluate the material's intrinsic properties after erasing its thermal history. In both the first and second heating scans, no notable changes were observed in the T_g of the PLA films on addition of CNC, irrespective of the blending technique. Intermolecular interaction and chain flexibility can cause a change in a material's T_g [38]. As expected, the low concentration of added CNCs did not significantly change the PLA's chain flexibility nor intermolecular interaction and consequently had no noteworthy effect on its T_g. In contrast, the T_c values of direct DB and MB PLNCNC films in the first and second heating scans were significantly lower than that of neat PLA (control films), indicating faster crystallization due to the nucleation effect of CNCs, as expected from the heterogeneous nucleation theory [39]. The nucleation rate (N), according to the heterogeneous nucleation theory is given as follows [39]:

$$N \cong N_o \times \exp\left(\frac{-C}{\Delta T}\right) \quad (4)$$

where N_o is the pre-factor, and ΔT and C are given as follows:

$$\Delta T = T_m^o - T_c \quad (5)$$

$$C = \frac{4 \cdot \sigma \cdot \sigma_e \cdot T_m^o}{k \cdot T \cdot \Delta h} \quad (6)$$

where T is the equilibrium melting temperature, Tc is the cold crystallization temperature, 6 and o_{σ} are the end and lateral surface free energies, k is the Boltzmann's constant, T is the temperature and $l/i.h$ is the enthalpy of fusion.

As *Eq.* (4) and (5) suggest, a lower cold crystallization temperature results in higher nucleation rate and faster crystallization. Thus, the lower Tc of PLNCNC composite films obtained in this study was accompanied by significantly higher crystallinity compared to neat PLA films in the second heat curve confirming that CNCs acted as efficient nucleating agents. Similar results have been reported for PLA nanocomposites with CNCs [17, 34, 40-42], microcrystalline cellulose (MCC) [43], cellulose nanofibers [44], and plasticized PLA with MCC [16]. It is also worth mentioning that a significantly lower T_c was observed for the melt-blended (MB) PLNCNC films compared to their direct DB counterparts because of the faster crystallization of shorter polymer chains resulting from degradation of the MB PLNCNC films, leading to a lower T_c. However, this reduced T_c, indicating nucleating action of the degradation products in the MB films was not accompanied by a further increase in crystallinity. GPC (described in the next section) was performed to confirm the degradation of MB PLNCNC films. The T_m of direct DB PLNCNC films remained unchanged as compared to neat PLA in the first and second heating curves. In contrast, the MB PLA/CNC films had a significantly lower T_m, which was attributed to the degradation of these films. Generally, degradation of films is accompanied by a reduction in molecular weight leading to reduced chain length and chain entanglement. Shorter and less entangled chains require less energy to slide past each other and melt at lower temperatures.

Effects of CNC Addition and Blending Process on the Degradation of PLA

As discussed above, the T_c and T_m results (Table 1) revealed that the extra heat and mechanical shear experienced in the MB process degraded the MB PLNCNC films. GPC was performed to evaluate PLA degradation of films and the results are shown in Table 2. The addition of CNCs through the direct DB process did not affect the Mn of PLA films, whereas their addition through the MB process decreased the M_n of PLA films. The mechanical shear generated at 22,000 rpm during the direct DB process had no significant effect on the M_n of direct DB *PLN* CNC compounds. However, the M_n of PLNCNC films produced by the MB process was significantly lower than their direct DB counterparts and neat PLA, which can be attributed to the additional heat exposure of these compounds during the MB

TABLE 2. Molecular weights of PLA films and PLNCNC films as well as unblended neat PLA pellets and neat PLA pellets subjected to direct dry- (DB) and melt-blending (MB) processes.

Materials	M_n (kg/mol)	M_w (kg/mol)	M_v (kg/mol)	# Chain scission (10^{-6} mol/kg)
Films				
PLA	142 ± 3[a]	272 ± 10[a]	252 ± 8[o]	-
PLA + 1% CNC (DB)	138 ± 3[a]	272 ±4[a]	251 ± 4[a]	213
PLA + 1% CNC (MB)	126 ±7[b]	267 ± 13[a]	246 ± 11[a]	915
Pellets				
PLA	158 ± 7[a]	310 ± 13[a]	287 ± 12[a]	-
PLA (DB)	147 ± 11[a]	299 ± 7[a,b]	276± 7[a]	509
PLA (MB)	130 ± 9[b]	282 ± 17[b]	259± 15[b]	1399

Same superscript letters within the same column of films or pellets are not significantly different based on the ANOVA results at 5% significance level.

DOI 10.1002/pen

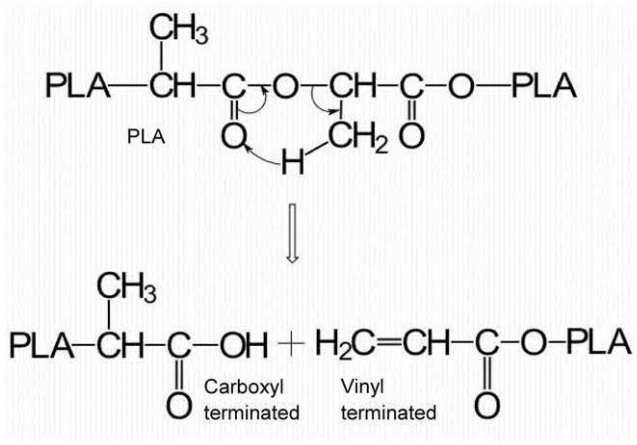

FIG. 4. Proposed β-C-H transfer mechanism for degradation of PLA.

process in a three-piece mixer prior to blown film extrusion. To verify that more degradation occurred during the MB process prior to blown film extrusion, neat PLA pellets were blended through direct DB and MB approaches and their average molecular weights determined. The degradation of direct DB and MB neat PLA pellets during compounding followed similar trends to that obtained with PLNCNC films (Table 2). The MB process was more deleterious to the degradation of PLA pellets than the direct DB process.

The degradation of PLA is very complex and can occur by various mechanisms, including random main chain scission reactions and hydrolysis (36, 37, 45]. Hydrolytic degradation results in drastic reduction in average molecular weight. Nevertheless, since the reduction in Mn was not very prominent, the dominating mechanism of degradation was more likely to be chain scission and not hydrolysis (36]. The number of chain scissions for the PLA/CNC composite films was calculated using the following *Eq.* (46,47]:

$$\#\text{chain scissions} = \frac{1}{M_n(\text{composite})} - \frac{1}{M_n(\text{PLA})} \quad (7)$$

where M_n (composite) is the number average molecular weight of PLA/CNC (DB) or PLA/CNC (MB) films and M_n (PLA) is the number average molecular weight of PLA films. The chain scissions in PLA pellets without any CNCs exposed to direct DB and MB conditions were also calculated using *Eq.* 7, where M_n (composite) represents the M_n of PLA (DB) or PLA (MB) and M_n (PLA) is the M_n of unblended PLA pellets.

Unsurprisingly, the PLA/CNC MB films and neat melt-blended PLA pellets (MB) had more chain scissions compared to their direct DB counterparts, indicating that the MB composites degraded more during the MB process as expected (Table

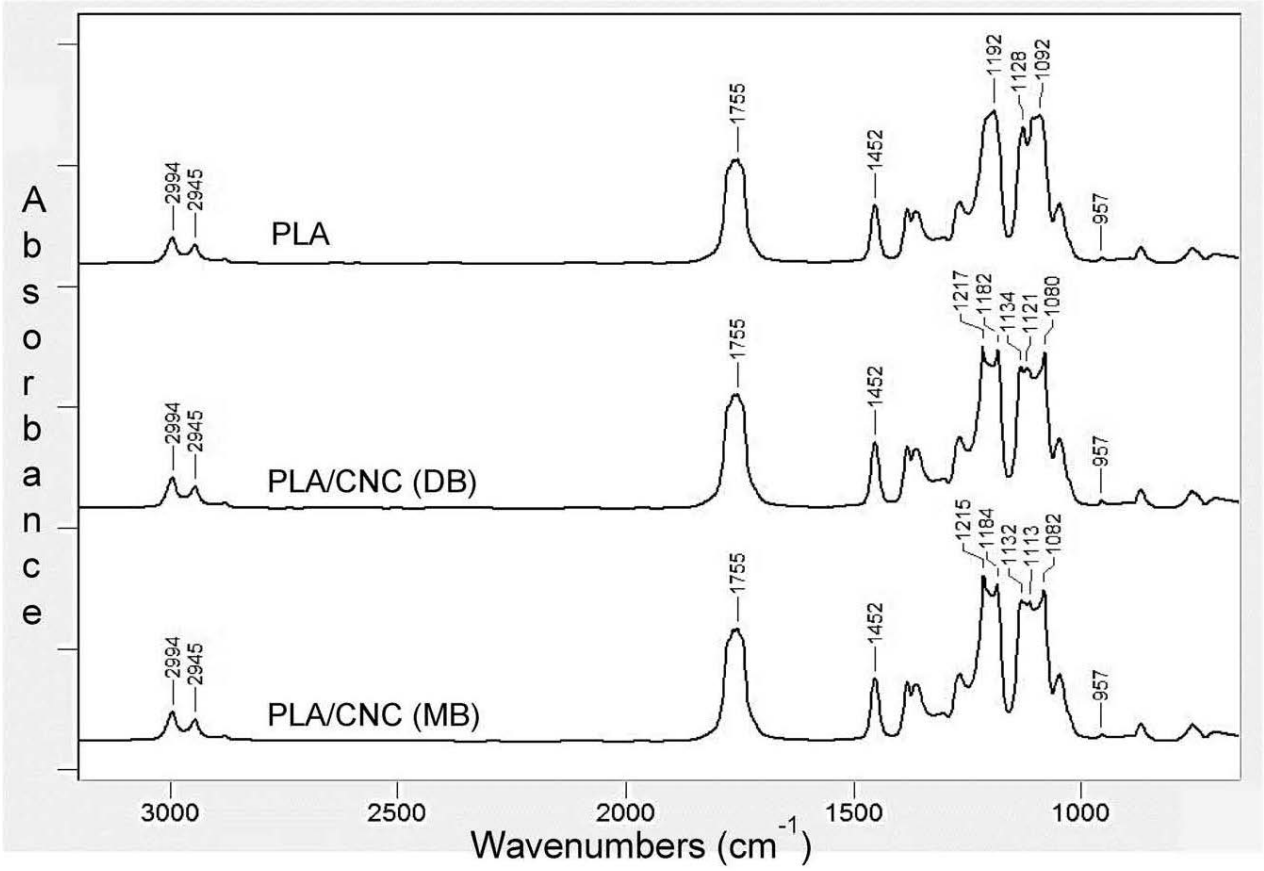

FI G. 5. Infrared spectra of PLA and PLN CNC composite films prepared by direct dry-blending (DB) and melt-blending (MB) processes.

TABLE 3. Band assignments for the wavenumbers of peaks used in FTIR analysis and corresponding functional groups [6, 36, 50-55].

Wavenumber (cm-!)			
PLA	PLNCNC (DB)	PLNCNC (MB)	Peak assignments
2994, 2945	2994, 2945	2994, 2945	Stretching of C-H in CH_3
1755	1755	1755	Stretching of C=O
1452, 1382, 1364	1452, 1382, 1364	1452, 1382, 1364	Stretching of C-H in CH_3
1267, 1192, 1128, 1092, 1047	1267, 1217, 1182, 1134, 1121, 1080, 1047	1267, 1215, 1184, 1132, 1113, 1082, 1047	Stretching of C-O in carboxyl and C-O-C stretch
957	957	957	O–H vibration in carboxyl
870	870	870	Amorphous phase of PLA
756	756	756	Crystalline phase of PLA

2). These findings corroborate the T_c and T_m results (Table 1) that indicated degradation of the PLA/CNC MB composites.

It was of interest to further investigate the mechanism of degradation occurring in the PLA/CNC composite films. A literature review revealed that in case of polyesters, chain scission can occur via β-C-H transfer reaction (Fig. 4), leading to a decrease in molecular weight and generation of vinyl terminated ester and carboxyl end-group [36, 45, 48, 49]. The presence of carboxyl end-groups, which designates degradation, can be detected by FTIR spectroscopy [30, 31]. Infrared spectra of neat PLA and PLNCNC composite films prepared by both blending processes are shown in Fig. 5. Table 3 lists the band assignments for the wavenumbers of peaks found in these spectra to their corresponding functional groups [6, 36, 50-55].

The major differences between the spectrum of PLA film and the spectra of PLNCNC films were observed in the region between 1045 and 1270 cm^{-1}, associated with C-O and C-O-C stretching. The peak present at 1192 cm^{-1} in neat PLA split into two peaks at 1217 and 1182 cm^{-1} in the PLA/CNC (DB) films, and 1215 and 1184 cm^{-1} in the PLA/CNC (MB) films. Additionally, the sharp peak at 1128 cm^{-1} in PLA films split into two broader peaks in the composite films (1134 and 1121 cm^{-1} in PLNCNC [DB]; 1132 and 1113 cm^{-1} in PLA/CNC [MB]). The broad peak in PLA at 1092 cm^{-1} became sharper and shifted to lower wavelengths in the range of 1080-1082 cm^{-1} for the composite films. These changes could indicate degradation of the PLNCNC composite films because ester linkages in PLA's main chain cleave to form carboxyl end-groups, as illustrated in Fig. 4. However, since the region between 1045 and 1270 cm^{-1} is assigned to both, C-O stretch from carboxyl groups and C-O-C stretching vibrations, it was difficult to use its intensity or area to accurately quantify the formation of carboxyl end-groups. Thus, the intensity of the peak at 957 cm^{-1}, assigned specifically to the O-H vibrations in carboxyl groups, was considered more appropriate to monitor the carboxyl group formation by calculating the carboxyl index (*Eq. 2*). An increase in carboxyl index would indicate the presence of additional carboxyl end-groups generated due to main chain scission by the proposed degradation mechanism (Fig. 4).

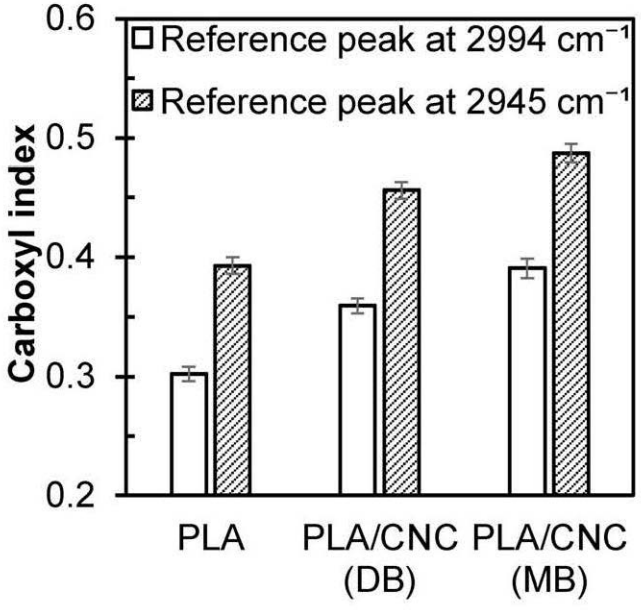

FIG. 6. Carboxyl indices using the intensities of reference peaks at 2994 and 2945 cm^{-1} of PLA, PLA/1% CNC (DB) and PLA/1% CNC (MB) films .

The carboxyl indices of PLA and PLA/CNC composite films are illustrated in Fig. 6. PLA/CNC composite films have higher carboxyl indices compared to PLA, indicating that chain scission occurred during both, the direct DB and MB processes by the proposed degradation mechanism (Fig. 4). However, the PLA/CNC MB films have higher carboxyl index than their direct DB counterparts suggesting that more chain scissions occurred for these films, in corroboration with the GPC results.

Effects of CNC Addition and Blending Process on the WVTR and OTR of PLA

The incorporation of 1% CNCs into the PLA matrix improved its water and oxygen barrier performance, irrespective of the blending process (Table 4). This improved barrier performance of

TABLE 4. WVTR and OTR of PLA as well as direct dry-blended (DB) and melt-blended (MB) PLA/1% CNC films.

	WVIR at 38°C and 85% RH (10^{-8} kg/m^2 s)		OTR at 23°C and 0% RH (10^{-10} kg/m^2 s)	
Materials	Average	% Decrease	Average	% Decrease
PLA	584.9 ± 49.5[a]	–	442.3 ± 87.4[a]	
PLA+ 1% CNC (DB)	409.7 ± 21.3[b]	30	178.9 ± 23.1[b]	60
PLA+ 1% CNC (MB)	442.9 ± 25.9[c]	24	270.1 ± 77.4[c]	39

Sarne superscript letters within the same column are not significantly different based on the ANOVA results at 5% significance level.

DOI 10.1002/pen

PLA/CNC composite films can be attributed to the presence of highly crystalline cellulose nanocrystals which act as impermeable regions in the matrix. The impermeable regions create a more tortuous diffusion path for the permeant, leading to slower diffusion and hence lower transmission rates [2, 56, 57].

Nonetheless, it should be mentioned that the WVTR and OTR of PLA/CNC MB films was higher than their direct DB counterparts due to thermal degradation of these films as demonstrated by DSC (Table 1), GPC (Table 2), and FTIR (Fig. 6) results. From obtained WVTR and OTR results, direct DB appeared to be the better approach for incorporating CNCs into the PLA matrix to enhance its water and oxygen barrier properties.

CONCLUSIONS

Two different approaches of incorporating CNCs into a PLA matrix were examined. The first method involved the MB of PLA and CNCs in a three-piece internal mixer for homogenous dispersion of CNCs into the matrix. The second method, direct DB, consisted of direct dry-mixing of PLA and CNCs in a high intensity mixer. The compounded materials were then blown into films and compared in terms of particle dispersion, optical, thermal, molecular weight and barrier properties. Based on the experimental results, the following conclusions were drawn:

1. The distribution and dispersion of CNCs were not influenced by the blending method. Good distribution of CNCs was achieved in the PLA matrix but some agglomerations were still visible, indicative of not well-dispersed CNCs in the matrix, irrespective of the blending process. Poor dispersion negatively impacted the transparency of PLNCNC composite films. Nevertheless, composite films with 75%-78% transmission were obtained, demonstrating that reasonably good transparency remains despite limited dispersion.
2. Overall, PLNCNC composite films produced by both direct DB and MB approaches thermally degraded during the blending process, but at different extents. The degradation was demonstrated and quantified using various analytical methods such as GPC, FTIR, and DSC, which clearly indicated that the PLNCNC MB films degraded more than their direct DB counterparts. The β-C-H transfer appeared to be the dominant mechanism of degradation for the composite films.
3. The incorporation of CNCs into the PLA matrix by the direct DB and MB processes improved the water vapor barrier properties of unfilled PLA films by 30% and 24%, respectively and oxygen barrier properties by 60% and 39%, respectively. The inferior barrier performance of the PLA/CNC MB films compared to the direct DB counterpart films could be attributed to the thermal degradation caused by the extra heat exposure of the compound during the MB process in a three-piece mixer prior to blown film extrusion.

In conclusion, the direct DB technique appeared to be the better approach for incorporating CNCs into the PLA matrix because it exposes the samples to less heat and thus minimizes thermal degradation.

ACKNOWLEDGMENTS

We gratefully acknowledge The U.S. Endowment for Forestry and Communities, Inc. - The Public-Private Partnership for Nanotechnology (P3Nano Grant No. P3-8b) for financial support of this research work. We also thank Mcintire Stennis for additional financial support and Richard S. Reiner (USDA Forest Service, Forest Products Laboratory) for preparing the CNCs.

REFERENCES

1. K. Oksman, M. Skrifvars, and J.F. Selin, *Compos. Sci. Technol.,* **63**, 1317 (2003).
2. L.M. Matuana, S.S. Karkhanis, N.M. Stark, and R.C. Sabo, *Biotech, Biomater. Biomed. - Tech. Connect Briefs,* **3,** 1 (2016).
3. K.A. Afrifah and L.M. Matuana, *Macromol. Mater. Eng.,* **297,** 167 (2012).
4. K.A. Afrifah and L.M. Matuana, *Macromol. Mater. Eng.,* **295,** 802 (2010).
5. S. Vijayarajan, S.E.M. Selke, and L.M. Matuana, *Macromol. Mater. Eng.,* **299,** 622 (2014).
6. C. Xing and L.M. Matuana, *J. Appl. Polym. Sci.,* **133,** 43201 (2016).
7. S.S. Karkhanis, N.M. Stark, R.C. Sabo, and L.M. Matuana, *J. Appl. Polym. Sci.,* **134**, 45212 (2017).
8. B. Mallet, K. Lamnawar, and A. Maazouz, *Polym. Eng. Sci.,* **54**, 840 (2014).
9. M. Mihai, M.A. Huneault, and B.D. Pavis, *Polym. Eng. Sci.,* **50**, 629 (2010).
10. N. Najafi, M.C. Heuzey, and P.J. Carreau, *Polym. Eng. Sci.,* **53**, 1053 (2013).
11. K.S. Chun, S. Husseinsyah, and H. Osman, *Polym. Eng. Sci.,* **53,** 1109 (2013).
12. N. Tripathi, Monika and V. Katiyar, *Polym. Eng. Sci.,* DOI 10.1002/pen.24497 (2017).
13. A. Arias, M.C. Heuzey, M.A. Huneaul,t G. Ausias, and A. Bendahou, *Cellulose,* **22,** 483 (2015).
14. M. Jonoobi, J. Harun, A.P. Mathew, and K. Oksman, *Compos. Sci. Technol.,* 70, 1742 (2010).
15. A.P. Mathew, G. Gong, N. Bjorngrim, D. Wixe, and K. Oksman, *Polym. Eng. Sci.,* **51,** 2136 (2011).
16. K. Halasz and L. Csoka, *J. Eng.,* **2013,** 1 (2013).
17. Q. Shi, C. Zhou, Y. Yue, W. Guo, Y. Wu, and Q. Wu, *Carbohydr. Polym.,* **90,** 301 (2012).
18. E. Fortunati, M**.** Peltzer, I. Armentano, L. Torre, A. Jimenez, and J.M. Kenny, *Carbohydr. Polym.,* **90,** 948 (2012).
19. A. Pei, Q. Zhou, and L.A. Berglund, *Compos. Sci. Technol.,* **70**, 815 (2010).
20. N. Herrera, A.P. Mathew, and K. Oksman, *Compos. Sci. Technol.,* **106,** 149 (2015).
21. N. Herrera, N, A.M. Salaberria, A.P. Mathew, and K. Oksman, *Compos. Part A. Appl. Sci. Manuf,* **83,** 89 (2016).
22. N. Herrera, H. Roch, A.M. Salaberria, M.A. Pino-Orellana, **J.** Labidi, S.C. Fernandes, D. Radie, A. Leiva, and K. Oksman, *Mater. Des.,* **92**, 846 (2016).
23. D. Bondeson and K. Oksman, *Compos. Part A. Appl. Sci. Manuf.,* **38,** 2486 (2007).
24. J.W. Rhim, A.K. Mohanty, S.P. Singh, and P.K. Ng, *J. Appl. Polym. Sci.,* **101,** 3736 (2006).
25. O. Faruk and L.M. Matuana, *Compos. Sci. Technol.,* **68,** 2073 (2008).

26. R.S. Reiner, and A.W. Rudie, *Production and Applications of Cellulose Nanomaterials,* TAPPI Press, Peachtree Comers, pp. 21-24 (2013).
27. M.T. Postek, A. Vladar, J. Dagata, N. Farkas, B. Ming, R. Wagner, A. Raman, R.J. Moon, R. Sabo, and T.H. Wegner, *Meas. Sci. Technol.,* **22**, 1 (2011).
28. A. Nuzzo, S. Coiai, S.C. Carroccio, N.T. Dintcheva, C. Gambarotti, and G. Filippone, *Macromol. Mater. Eng.,* **299,** 1 (2014).
29. D. Battegazzore, S. Bocchini, and A. Frache, *Express. Polym. Lett.,* **5,** 849 (2011).
30. N.M. Stark and L.M. Matuana, *Polym. Degrad. Stab.,* **86**, 1 (2004).
31. G.J.M. Fechine, M.S. Rabello, R.S. Maior, and L.H. Catalani, *Polymer,* **45**, 2303 (2004).
32. S.E.M. Selke and J.D. Cutler, *Plastics Packaging: Properties, Processing, Applications and Regulations,* Hanser Publications, Cincinnati, pp. 159-184 (2016).
33. Y. Zhou, C. Fuentes-Hernandez, T.M. Khan, J.C. Liu, J. Hsu, J.W. Shim, A. Dindar, J.P. Youngblood, R.J. Moon, and B. Kippelen, *Sci. Rep.,* **3,** 1 (2013).
34. E. Lizundia, E. Fortunati, F. Dominici, J.L. Vilas, L.M. Leon, I. Armentano, L. Torre, and J.M. Kenny, *Carbohydr. Polym.,* **142,** 105 (2016).
35. Y. Wang, B. Steinhoff, C. Brinkmann, and I. Alig, *Polymer,* **49**, 1257 (2008).
36. R. AI-Itry, K. Lamnawar, and A. Maazouz, *Polym. Degrad. Stab.,* **97**, 1898 (2012).
37. K. Jamshidi, S.H. Hyon, and Y. Ikada, *Polymer,* **29,** 2229 (1988).
38. L.H. Sperling, *Introduction to Physical Polymer Science,* John Wiley & Sons Publication, New Jersey, pp. 349---426 (2006).
39. E. Piorkowska and G.C. Rutledge, *Handbook of Polymer Crystallization,* John Wiley & Sons Publication, New Jersey, pp. 125-163 (2013).
40. I. Cacciotti, E. Fortunati, D. Puglia, J.M. Kenny, and F. Nanni, *Carbohydr. Polym.,* **103,** 22 (2014).
41. E.M. Sullivan, R.J. Moon, and K. Kalaitzidou, *Materials,* **8,** 8106 (2015).
42. A. Gupta, W. Simmons, G.T. Schueneman, D. Hylton, and E.A. Mintz, *ACS. Sustain. Chem. Eng.,* **5**, 1711 (2017).
43. A.P. Mathew, K. Oksman, and M. Sain, *J. Appl. Polym. Sci.,* **101,** 300 (2006).
44. X. Wang, C. Bai, J. Zhang, A. Sun, X. Wang, and D. Wei, *Bio-Resources,* **1,** (2014).
45. F.D. Kopinke, M. Remmler, and K. Mackenzie, *Polym. Degrad. Stab.,* **52,** 25 (1996).
46. D. Rasselet, A. Ruellan, A. Guinault, G. Miquelard-Garnier, C. Sollogoub, and B. Fayolle, *Eur. Polym. J.,* **50,** 109 (2014).
47. O. Saito, *J. Phys. Soc. Jpn.,* **13**, 1451 (1958).
48. BJ. Holland, and J.N. Hay, *Polymer,* **43**, 1835 (2002).
49. Y. Aoyagi, K. Yamashita, and Y. Doi, *Polym. Degrad. Stab.,* **76**, 53 (2002).
50. X. Liu, Y. Zou, W. Li, G. Cao, and W. Chen, *Polym. Degrad. Stab.,* **91,** 3259 (2006).
51. K. Carlbom and L.M. Matuana, *Polym. Composite,* **26,** 534 (2005).
52. K. Carlbom andLM. Matuana, *Polym. Composite,* **27**, 599 (2006).
53. K. Carlbom and L.M. Matuana, *J. Appl. Polym. Sci.,* **101,** 3131 (2006).
54. Q. Li and L.M. Matuana, *J. Appl. Polym. Sci.,* **88,** 278 (2003).
55. J. Palacios, C. Albano, G. Gonzalez, R.V. Castillo, A. Karam, and M. Covis, *Polym. Eng. Sci.,* **55**, 710 (2015).
56. J. George and S.N. Sabapathi, *Nanotechnol. Sci. Appl.,* **8,** 45 (2015).
57. N.M. Stark, *J. Renew. Mater.,* **4**, 313 (2016).

 DOI 10.1002/pen